pubs.acs.org/Biomac

Article

Controlled Release of Exosomes Using Atom Transfer Radical Polymerization-Based Hydrogels

Saigopalakrishna S. Yerneni, Sushil Lathwal, Julia Cuthbert, Kriti Kapil, Grzegorz Szczepaniak, Jaepil Jeong, Subha R. Das,* Phil G. Campbell,* and Krzysztof Matyjaszewski*

Cite This: *Biomacromolecules* 2022, 23, 1713−1722

Read Online

ACCESS | Metrics & More | Article Recommendations | Supporting Information

ABSTRACT: Exosomes are 30−200 nm sized extracellular vesicles that are increasingly recognized as potential drug delivery vehicles. However, exogenous exosomes are rapidly cleared from the blood upon intravenous delivery, which limits their therapeutic potential. Here, we report bioactive exosome-tethered poly(ethylene oxide)-based hydrogels for the localized delivery of therapeutic exosomes. Using cholesterol-modified DNA tethers, the lipid membrane of exosomes was functionalized with initiators to graft polymers in the presence of additional initiators and crosslinker using photoinduced atom transfer radical polymerization (ATRP). This strategy of tethering exosomes within the hydrogel network allowed their controlled release over a period of 1 month, which was much longer than physically entrapped exosomes. Exosome release profile was tuned by varying the crosslinking density of the polymer network and the use of photocleavable tethers allowed stimuli-responsive release of exosomes. The therapeutic potential of the hydrogels was assessed by evaluating the osteogenic potential of bone morphogenetic protein 2-loaded exosomes on C2C12 and MC3T3-E1 cells. Thus, ATRP-based exosome-tethered hydrogels represent a tunable platform with improved efficacy and an extended-release profile.

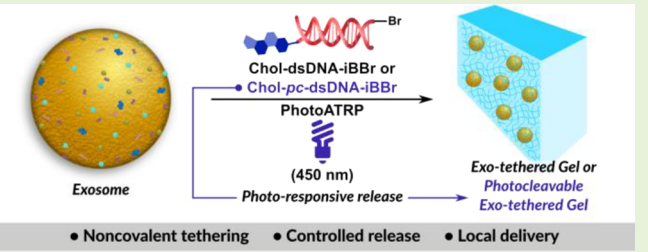

INTRODUCTION

Exosomes, a subclass of cell-derived extracellular vesicles, play a vital role in intercellular communication throughout life, both in health and disease.[1] Their biogenesis, small size of 30−200 nm, biocompatibility, and ability to carry biological cargos including nucleic acids, proteins, and lipids have prompted their exploration as drug delivery vehicles.[2,3] Moreover, exosomes have been increasingly seen as a replacement for stem cell therapies owing to their endogenous cargo.[4] Encapsulation of both endogenous and exogenous therapeutic agents in the lumen of exosomes protects them from inactivation within the extracellular environment via enzymatic degradation and/or by their antagonists.[5,6] Moreover, codelivery of native cargos, such as miRNA, could possibly augment the therapeutic efficacy of exosomes.[7,8] While exosomes provide several advantages over synthetic drug delivery systems, such as liposomes, lipid nanoparticles, and polymer micelles, their clinical success has been limited.[9,10] Exosomes are known to be rapidly cleared from the blood after systemic administration in vivo.[11] As large-scale production of exosomes is not easy to achieve and a matter of intense research at present, using higher doses of exosomes to counteract their clearance is a major bottleneck for clinical translation of exosome-based therapeutics.[12] Another alternative to systemic administration of exosomes, where appropriate, is their local administration using macroscale delivery systems, like hydrogels. These systems facilitate higher bioavailability of an included therapeutic at the intended site with minimal off-target side-effects.[13,14]

Hydrogels have a high water content, and their porous nature can be further tuned through crosslinking density. These characteristics make hydrogels biological tissue-like in terms of their mechanical stiffness and biocompatibility. Therefore, hydrogels have been extensively studied for the delivery of small molecules, proteins, and cells for biomedical applications.[15−17] Some recent reports on hydrogels for exosome delivery rely on the use of natural polymers based on polypeptides and polysaccharides such as chitosan, silk fibroin, alginate, hyaluronic acid, and others.[18,19] Although these polymer matrices for hydrogels provide favorable biocompatibility and biodegradation, the use of synthetic polymers for exosome entrapment has not been well explored.[20] Synthetic polymers can afford highly tunable frameworks through monomer (+comonomer) choice, molecular weights, and crosslinking density and thereby provide

Received: December 15, 2021
Revised: March 10, 2022
Published: March 18, 2022

https://doi.org/10.1021/acs.biomac.1c01636
Biomacromolecules 2022, 23, 1713−1722

better control over physical properties like swelling, elasticity, and porosity. These advantages of synthetic polymers led us to explore their use as a potential local delivery system for exosomes.

New developments in the field of reversible deactivation radical polymerization (RDRP) further allow ambient polymerization conditions, low radical concentration to avoid damage of biological cargos, uniform pore size for controlled release, and access to postsynthesis modifications.[21−26] Atom transfer radical polymerization (ATRP) is a powerful and versatile RDRP process.[27−29] It can be carried out in a variety of solvents, at different temperatures, including under biorelevant conditions. ATRP offers tunable polymerization conditions and parameters that provide control over reaction kinetics. In addition to heterogeneous and homogeneous solution polymerization, polymers can be grown from a variety of biomolecules, such as DNA, RNA, sugars, and proteins, including nanoparticles. We recently reported "grafting-to" and "grafting-from" strategies to engineer a novel class of drug carriers called exosome-polymer hybrids.[7] Expanding upon the "grafting-from" strategy, here we report engineering of exosome-tethered hydrogels.

EXPERIMENTAL SECTION

Exosome Isolation and Characterization. Exosomes from conditioned media were isolated by size exclusion chromatography (SEC) using a previously described protocol.[30−33] Briefly, conditioned media (minimum of 48 h in cell culture) were differentially centrifuged (2000 g for 10 min at 4 °C and 10,000 g for 30 min at 4 °C) followed by ultrafiltration (0.22 μm filter; Millipore-Sigma, Billerica, MA) and then SEC on an A50 cm column (Bio-Rad Laboratories, Hercules, CA, USA) packed with Sepharose 2B (Sigma-Aldrich, St. Louis, MO, USA). Protein concentrations of exosome fractions were determined using a BCA protein assay kit as recommended by the manufacturer (Pierce, Thermo Fisher Scientific). Further characterization of exosomes was done with tunable resistive pulse sensing, western blotting, and transmission electron microscopy. See SI Appendix for detailed procedures.**

DNA Synthesis. All DNA sequences were either synthesized using a MerMade4 DNA synthesizer (Bioautomation, Irving, TX) using the standard DNA phosphoramidites (ChemGenes, Wilmington, MA) or ordered from IDT (Integrated DNA Technologies, Inc., Iowa, USA). Commercially available phosphoramidites (Glen Research, Sterling, VA) were used to introduce modifications on the 3′-end and 5′-end during the DNA synthesis. DNA macroinitiator sequences (DNA′-iBBr) were synthesized by coupling α-bromoisobutyrate initiator phosphoramidite on the 5′-end as previously reported.[34] See SI Appendix for more details.

Preparation and Characterization of Bone Morphogenetic Protein 2 (BMP2)-Loaded Exosomes. Loading of BMP2 into exosomes was performed by adopting a previously reported protocol.[6,35] A mixture of 10 μg of exosomes and 1 μg of BMP2 was sonicated (Tekmar sonic disruptor) on ice using a 0.25″ tip at 20% amplitude, 6 cycles of 30 s on/off for 3 min with a 2 min cooling period between each cycle. The unloaded BMP2 was removed using a 100,000 kDa MWCO membrane filter (Vivaspin columns, Sartorius AG, Göttingen, Germany) followed by SEC. Exosome surface-bound BMP2 was removed by pH 3.0 acid-incubation, followed by separation of exosomes from BMP2 using SEC. To confirm the loading of BMP2 in exosomes, western blotting analysis was performed.

Preparation of the Exosome Macroinitiator. Chol-dsDNA-iBBr was prepared by annealing Chol-DNA and DNA′-iBBr strands using sequential incubation at 37, 0 °C, and room temperature for 15, 10, and 30 min, respectively. Then, 100 μL of native exosomes or BMP2-exosomes (0.4 μg/μL exosome concentration) was gently vortexed with 100 μL of preannealed Chol-dsDNA-iBBr tether (2 μM dsDNA tether concentration, followed by three washes with Amicon Ultra Centrifugal Filters (100 k MWCO). The filters were reverse spun to prepare 100 μL of Exo-dsDNA-iBBr (0.4 μg/μL exosome stock concentration, 1 μM initiator concentration). A similar process was followed to prepare photocleavable (*pc*) exosome macroinitiators using Chol-*pc*-DNA and DNA′-iBBr as the DNA tethers.

Preparation of Hydrogels by Atom Transfer Radical Polymerization. Plain hydrogels of a monomer-to-crosslinker ratio of 4000 were prepared without any exosomes or DNA macroinitiators. Molar ratios of different components were as follows: $[PEGMA_{300}]_0/[PEGDMA_{750}]_0/[PEO_{2000}\text{-iBBr}]_0/[CuBr2]_0/[TPMA]_0$ = 8000/2/1/1/6. Specifically, 400 μL of $PEGMA_{300}$ monomer, 87.5 μL of PEO_{2000}-iBBr (2 mM stock concentration), 23.6 μL of $PEGDMA_{750}$ (14.8 mM stock concentration), 14.6 μL of $CuBr_2$/TPMA (12 mM stock concentration; $CuBr_2$/TPMA = 1:6), 20 μL of glucose oxidase (100 μM stock concentration), 50 μL of sodium pyruvate (2 M stock concentration), and 100 μL of 10× phosphate buffer saline (PBS) buffer were thoroughly mixed with 204 μL of H_2O in a 4 mL glass vial. Finally, 100 μL of glucose (1 M stock concentration) was added to the vial followed by irradiation under blue light (450 nm, 5.4 mW/cm^2) for 120 min at room temperature.

Exosome-tethered hydrogels were prepared in the presence of exosome macroinitiators. Molar ratios of different components were as follows: $[PEGMA_{300}]_0/[PEGDMA_{750}]_0/[PEO_{2000}\text{-iBBr}]_0/[Exo\text{-}dsDNA\text{-}iBBr]_0/[CuBr2]_0/[TPMA]_0$ = 8000/2/1/0.05/1/6. Specifically, 400 μL of $PEGMA_{300}$ monomer, 87.5 μL of PEO_{2000}-iBBr (2 mM stock concentration), 23.6 μL of $PEGDMA_{750}$ (14.8 mM stock concentration), 14.6 μL of $CuBr_2$/TPMA (12 mM stock concentration; $CuBr_2$/TPMA = 1:6), 20 μL of glucose oxidase (100 μM stock concentration), 50 μL of sodium pyruvate (2 M stock concentration), and 100 μL of 10× PBS buffer were thoroughly mixed with 104 μL of H_2O in a 4 mL glass vial. Then, 100 μL of Exo-dsDNA-iBBr (0.4 μg/μL exosome stock concentration, 1 μM initiator concentration) was added and mixed thoroughly. Finally, 100 μL of glucose (1 M stock concentration) was added to the vial, followed by irradiation under blue light (450 nm, 5.4 mW/cm^2) for 120 min at room temperature.

For BMP2-exosome-tethered hydrogels, BMP2-loaded Exo-dsDNA-iBBr (40 μg of exosome, 4 μg of BMP2, 1 μM initiator concentration) was used instead of Exo-dsDNA-iBBr. Hydrogels were prepared using the same method as for exosome-tethered hydrogels described above. The photocleavable exosome-tethered hydrogels were prepared using photocleavable exosome macroinitiators (Exo-*pc*-dsDNA-iBBr). Molar ratios of different components and reaction conditions were the same as those used for exosome-tethered gels.

The respective hydrogels with monomer-to-crosslinker ratios of 400 and 8000 were prepared by varying the crosslinker amount in the above-mentioned conditions. For a monomer-to-crosslinker ratio of 400, 236 μL of $PEGDMA_{750}$ (14.8 mM stock concentration) was used to prepare the hydrogels. For a monomer-to-crosslinker ratio of 8000, 11.8 μL of $PEGDMA_{750}$ (14.8 mM stock concentration), was used to prepare the hydrogels. The same procedure was followed to prepare BMP2-exosome-tethered hydrogels. See SI Appendix for more details.

Characterization of Hydrogels. *Confocal Microscopy.* Hydrogels were incubated for 24 h in a PBS buffer following which imaging was performed. Imaging was performed using a Carl Zeiss LSM 880 confocal microscope with fixed settings across all of the experimental time points, and the images were analyzed using ZEN Black software (Carl Zeiss Microscopy, Thornwood, NY). See SI Appendix for more details.

Polymerization Kinetics. Polymerization kinetics were studied through the preparation of a plain hydrogel. The pregel solution was irradiated with blue light (5.4 mW/cm^2), and samples were collected after different time points. The samples were analyzed by nuclear magnetic resonance (NMR) for conversion (Bruker Ultrashield 500 MHz operating at 500 MHz for ^{1}H using D_2O as the solvent).

Elastic Modulus Measurements. The mechanical properties of the hydrogels were assessed using an Anton Paar MCR-302 rheometer fitted with a 25 mm diameter stainless-steel parallel plate tool. Disk-shaped samples with a thickness of 6−8 mm and diameter (D) = 12.5

https://doi.org/10.1021/acs.biomac.1c01636
Biomacromolecules 2022, 23, 1713−1722

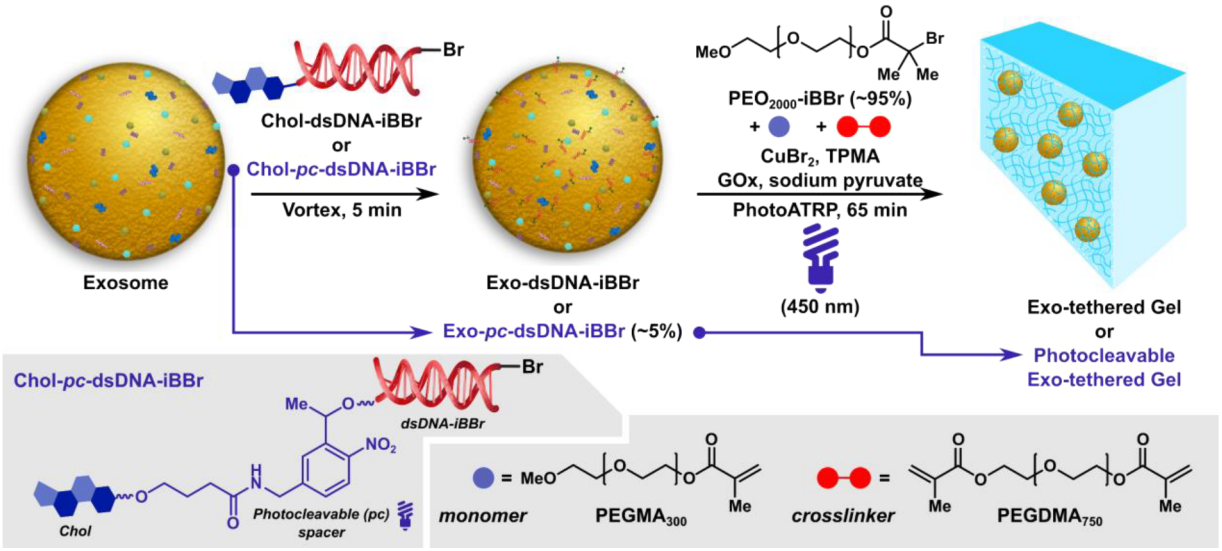

Figure 1. Preparation of exosome-tethered hydrogels. (Top) Exosome macroinitiator hybrids were prepared by tethering cholesterol and ATRP initiator-modified DNA tethers (Chol-dsDNA-iBBr) onto the exosome membrane. Hydrogels were prepared by grafting polymer chains from the exosome surface (Exo-dsDNA-iBBr; 5%) and in situ gelation using PEO-based initiators (PEO_{2000}-iBBr; 95%), a monomer, and a crosslinker using O_2-tolerant PhotoATRP. A *p*-nitrophenyl group was incorporated in DNA tethers (Chol-*pc*-dsDNA-iBBr; inset (bottom left)) to prepare photocleavable (*pc*) exosome-tethered hydrogels. The structures of the monomer and crosslinker are shown in the inset (bottom right).

mm were subjected to a normal load increasing linearly in time (loading rate = 0.1 N/s) from 0.1 to 5 N. The load vs distance curves were converted into the stress $\sigma = F/(\pi \times (D/2)2)$ and compression strain $\varepsilon = (d_0 - d)/d_0$, where the initial distance between the plates, d_0 (corresponding to the initial sample thickness), was determined by the extrapolation to zero load. Young's modulus (E) was calculated as the slope of the initial linear region of the constructed stress−strain curves. When testing the gel samples containing the photocleavable linker, the lights in the room were turned off.

Cytotoxicity and Cell Proliferation Assay. Cytotoxicity was assessed using direct CyQUANT nucleic acid-sensitive fluorescence assay (Thermo Fisher Scientific, Waltham, MA, USA) according to the manufacturer's instructions as described previously.[36,37] Briefly, 100 μL aliquots of HEK293 cell suspension containing 1×10^6 cells were plated in wells of a 6-well tissue culture plate (Corning Inc., Corning, NY, USA) and allowed to adhere for 8 h. Then, 0.8 g of gels (wet wt.) with and without 9.2 μg of tethered exosomes was added to respective treatment wells and coincubated with cells for 72 h. Sodium azide (5%) was used as a negative control and induced cell death. Gels with and without tethered exosomes were added to respective treatment wells and coincubated with cells for 72 h. At varying time points, the cells were labeled with CyQUANT Direct and fluorescence intensities measured with a TECAN spectrophotometer reader (TECAN, Männedorf, Switzerland). Cytotoxicity was assessed by normalizing fluorescence intensities to nontreatment control groups and plotted as percent viability.

Release Kinetic Studies. BMP2 was iodinated via a chloramine T method.[6] BMP2 (10 μg) was reacted with 500 μCi ^{125}I-Na at 25 °C with a stepwise addition of 3 aliquots of dilute chloramine T solution (100 μg/mL). Resulting ^{125}I-BMP2 was >97% trichloroacetic acid perceptible with minimal protein aggregate formation. The specific activity of ^{125}I-BMP2 was in the range of 55−80 μCi/μg. Exosomes were loaded with ^{125}I-BMP2 as described above. To label exosomes, a modified chloramine T method was employed.[38] Hydrogels were prepared as described above incorporating 10 μg of exosomes with or without ^{125}I-BMP2. Release kinetics were assessed in simulated body fluid (SBF; 10% FBS, 0.02% sodium azide, 25 mM HEPES in DMEM). Briefly, the hydrogels were put in 12 × 75 mm polypropylene tubes containing a total volume of 1 mL of SBF. The tubes were incubated at 37 °C, and at indicated time points, SFB was replaced and the retained ^{125}I-BMP2/^{125}I-exosomes were detected using a Wizard2 2-Detector Gamma Counter (PerkinElmer, Waltham, MA). On the 25th day, the hydrogels with photocleavable tethers were irradiated using 365 nm LEDs (50 mW/cm^2) for 2 min.

Exosome Membrane Integrity Experiments. The effect of hydrogel entrapment on exosome membrane integrity was assessed using a previously established technique that relies on intraluminal esterase activity in exosomes.[7,39] Calcein Deep Red (AAT Bioquest Inc., Sunnyvale, CA) was solubilized in DMSO and diluted with 1× PBS to a final concentration of 10 μM. Exosomes were isolated and labeled with calcein prior to incorporating them in the gels. To assess the membrane integrity of exosomes in the gels, fluorescence from calcein-labeled exosomes was measured using a TECAN spectrophotometer post hydrogel synthesis. To assess the membrane integrity of exosomes released from the gels, hydrogels were synthesized using Calcein Deep Red-labeled exosomes. Post synthesis, the gels were rinsed overnight in PBS and kept in 1 mL of PBS at 37 °C for 10 days. Post incubation, the collected PBS was concentrated down to 250 μL using 100 kDa M.W.C.O. filter, and fluorescence from calcein dye was assessed using on-bead flow cytometry using anti-CD63 conjugated magnetic beads as previously described.[40] CD63-conjugated magnetic beads (ExoCap, MBL International, Woburn, MA) were prepared as previously described.[40] Briefly, monoclonal anti-CD63 antibody (MA5−24169, Invitrogen, Carlsbad, CA) was biotinylated using a one-step antibody biotinylation kit purchased from Miltenyi Biotec (Auburn, CA) as recommended by the manufacturer. Biotinylated CD63 antibody (5 μg) was incubated with thoroughly washed 0.5 mL of streptavidin-coated magnetic beads (1×10^8 beads/mL) for 1 h at 25 °C under constant agitation. Then, 1 μg of nonprinted exosomes, bioprinted exosomes, and sonicated exosomes were each incubated with 100 μL of CD63-conjugated magnetic beads for 16 h at 4 °C under constant agitation. To assess membrane integrity, exosomes were captured on CD63 magnetic beads and washed three times with PBS, and 100,000 events/treatment were analyzed on an Accuri C6 flow cytometer (BD Biosciences, San Jose, CA) connected to an Intellicyt HyperCyt autosampler (IntelliCyt Corp., Albuquerque, NM) using a Cy5 channel (649 nm). Data were processed and interpreted using FlowJo software (FlowJo LLC, Ashland, Oregon).

Osteogenic Differentiation Studies. *Alkaline Phosphatase Assay.* Circular Exo-tethered hydrogels containing a total of 40 μg of exosomes were cut into four quadrants and rinsed thoroughly (four times) with 0.02% EDTA in PBS, the first wash being immediate, followed by three more rinses (4 h each). To treat the cells with the gel, the cells were plated in a 12-well plate and allowed to adhere

https://doi.org/10.1021/acs.biomac.1c01636
Biomacromolecules 2022, 23, 1713−1722

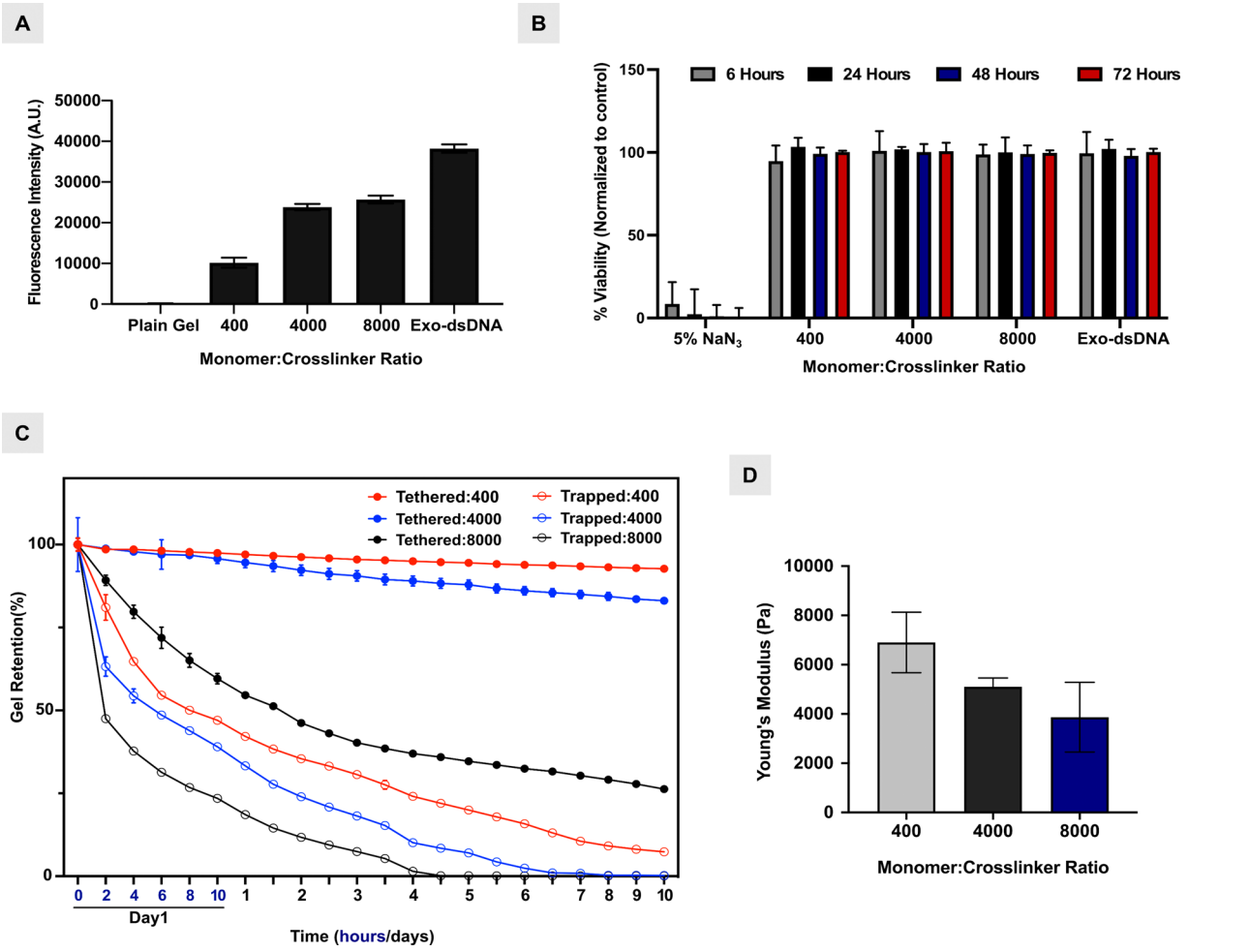

Figure 2. Characterization of exosome-tethered hydrogels. (A) Membrane integrity assessment of exosomes tethered/trapped in hydrogels with different monomer-to-crosslinker ratios. Bars indicate mean ± SEM (n = 4). (B) Effect of hydrogels with different monomer-to-crosslinker ratios on the cell viability and proliferation rate of HEK293 cells. (C) Exosome release kinetics (tethered/trapped) from different types of hydrogels measured using radiolabeled exosomes ^{125}I-exosomes. Points indicate mean ± SEM (n = 3 gels, two biological replicates). (D) Young's modulus of gels with different monomer/crosslinker ratios. Bars indicate mean ± SEM (n = 4).

overnight. For the treatments involving gels, 0.8 g of gel (wet wt.) was added to each well of a 12-well plate containing 5×10^5 cells per well. For every 0.8 g of gels, 9.2 μg of exosomes loaded with or without 190 ng of BMP2 was tethered. As controls, liquid-phase 100 ng/mL BMP2, 9.2 μg of native exosomes, and 9.2 μg of BMP2-exosomes were used. C2C12 cells were incubated with indicated treatments, washed with PBS to remove the culture medium, and fixed for 20 min with 10% neutral buffered formalin (Millipore-Sigma, St. Louis, MO). Alkaline phosphatase activity was detected using a leukocyte alkaline phosphatase assay kit according to the manufacturer's instructions (Millipore-Sigma, St. Louis, MO) as previously described.[6,41] Where required, alkaline phosphatase (ALP)-stained images were converted to the CMYK format since this color format is representative of reflected light colors as opposed to emitted light colors (RGB). Since the combination of cyan and magenta forms the color blue, these channels were added together and inverted. The average pixel intensity was determined using the image histogram tool in Adobe Photoshop 7.0 (Adobe Systems, San Jose, CA).

Mineralization. Exo-tethered hydrogels were cut like the ones used for the ALP assay. MC3T3-E1 (subclone 4) cells were seeded in growth media (ascorbic acid-free α-MEM, 10% FBS, 1% PS). For the treatment with hydrogels, the hydrogels were placed on the plated cells and the growth media supplemented with 50 μg/mL ascorbic acid and 10 mM β-glycerophosphate changed every 72 hrs. As a positive control, 100 ng/mL of BMP2 was added along with every change in media. On day 28, the cells were fixed in 10% neutral buffered formalin and washed with distilled water three times, and alizarin red stain (Millipore-Sigma, St. Louis, MO) was added to the wells and incubated for 1 h at room temperature. After imaging the cells, quantification of mineralization was performed using an osteogenesis quantitation kit (Millipore-Sigma, St. Louis, MO) according to the manufacturer's instructions. Briefly, alizarin red stained cells were treated with 10% acetic acid solution for 30 min with shaking, the cells were scraped and centrifuged, and the dissolved alizarin stain was quantified by measuring the OD at 405 nm (TECAN plate reader, Männedorf, Switzerland) using alizarin red reference standards.

RESULTS AND DISCUSSION

We previously reported that cholesterol-modified DNA tethers (Chol-DNA) can be used to rapidly functionalize exosomes with different functional moieties and polymers.[7,8] The negative charge of the DNA tether assists in outward orientation of the tethers. Further, the functionalization of the exosome surface through ATRP initiator-modified DNA tethers allows polymer chains to be directly grafted from the exosome by the "grafting-from" strategy.[7] Here, we combined the "grafting-from" strategy with "in situ gelation" to generate a polymer network that includes exosomes tethered through noncovalent interactions (Figure 1). Two short synthetic DNA

https://doi.org/10.1021/acs.biomac.1c01636
Biomacromolecules 2022, 23, 1713−1722

strands, one with a 5′-α-bromoisobutyrate group (DNA′-iBBr)[34] and another with a cholesterol (Chol-DNA), were annealed to prepare the ATRP initiator-functionalized double-stranded (ds) DNA tethers (Chol-dsDNA-iBBr) (Figure S1; Table S1). Exosomes were isolated from nonactivated macrophages J774A.1 and characterized with transmission electron microscopy, western blotting for protein markers, and the size distribution profile (Figure S2). As a comparison, we also isolated exosomes from THP1 cells (human leukemia monocytic cell line), which are our lab's gold standard for exosome isolation and characterization. The DNA tethers were gently vortexed with exosomes for 5 min at room temperature to generate exosome macroinitiator hybrids (Exo-dsDNA-iBBr) (Figure 1). Next, hydrogels were prepared using a 1:0.05 molar ratio of PEO_{2000}-iBBr and Exo-dsDNA-iBBr as initiators to allow a polymer framework based predominantly on PEO_{2000}-iBBr (95%), with the fewer polymer chains from Exo-dsDNA-iBBr (5%) acting as tethers for exosome entrapment. We selected poly(ethylene glycol) methacrylate (PEGMA, M_n = 300) as the monomer, poly(ethylene glycol) dimethacrylate (PEGDMA, M_n = 750) as the crosslinker, and $CuBr_2$/TPMA (TPMA = tris(2-pyridylmethyl)amine) as the catalyst. Hydrogels were prepared using photoinduced ATRP (PhotoATRP).[42] In PhotoATRP, upon light exposure, the Cu(II)/TPMA complex is reduced to a Cu(I)/TPMA activator when excess ligand is used. This photoreduction triggers polymerization. Hence, we chose blue LEDs (450 nm; 5.4 mW/cm^2) as the light source to avoid any damage to exosomes and the endogenous cargo.[22] Deoxygenation by physical degassing of the polymerization solution could damage the exosomes; hence, we used glucose oxidase (GOx), glucose, and sodium pyruvate as adjutants to convert dissolved oxygen to carbon dioxide during the polymerization reaction.[21,43] Further, a large monomer-to-crosslinker ratio (molar ratio) of 4000 (approximately 1 μm in length) was targeted to facilitate entrapment of exosomes. These polymerizations were performed in PBS (pH 7.4), and gelation was observed visually around 110 min of blue light exposure (Figures S3 and S4). To achieve temporal control over release of the exosomes tethered inside the polymer network, a photocleavable DNA tether (Chol-*pc*-DNA) was used; this incorporates a *p*-nitrophenyl group between the DNA and the cholesterol moiety (Figure 1, Figure S1, and Table S1). The photocleavable linker can be cleaved by a short (2 min) illumination with a UV (365 nm) light and is not affected by the blue (450 nm) light used for the polymerization process.[44,45]

The crosslinking density and resulting monomer-to-crosslinker ratio of the hydrogels can affect the membrane integrity of tethered exosomes due to physical crowding inside the polymer network. To assess this effect, we used Calcein Deep Red , an exosome-permeant dye that relies on intraluminal esterase activity and allows differentiation between intact exosomes and debris.[39] Calcein-labeled exosomes prepared using a previously described protocol[5] were used to make exosome-tethered hydrogels with three different monomer-to-crosslinker ratios of 400, 4000, and 8000. Hydrogels with monomer-to-crosslinker ratios of 4000 and 8000 showed a comparable fluorescence intensity at 650 nm (Figure 2A). However, the monomer-to-crosslinker ratio of 400 (approximately 100 nm in length) resulted in a very low exosome stability, and only 26% of the initial dye signal was observed. This decrease in calcein dye signal highlights that the membrane integrity of exosomes can get compromised in highly dense polymer networks.

The cytotoxicity of the exosome-tethered hydrogels was determined in HEK293 cells using the CyQuant assay. The hydrogels were prewashed (four times) with a PBS buffer containing 0.02% EDTA at 25 °C to remove the residual monomer before incubating with the cells for 72 h. The gels were made such that every 1 g of gel (wet wt.) contained 11.5 μg of exosomes. All exosome-tethered hydrogels with monomer-to-crosslinker ratios of 400, 4000, and 8000 showed no cytotoxic effects as shown in Figure 2B.

In addition to the crosslinking density of the polymer networks, entrapment strategies can play an important role in the release profile of cargos from the hydrogels. The release kinetics of tethered exosomes and physically entrapped (trapped) exosomes without any DNA-based tethers were compared using hydrogels of varying monomer-to-crosslinker ratios of 400, 4000, and 8000. To enable detection, exosomes were radiolabeled using ^{125}I, as described in the Experimental Section. The release kinetics were monitored over a period of 10 days (Figure 2C), and the retained radioactivity in the hydrogel was quantified at specific time points. For hydrogels with monomer-to-crosslinker ratios of 4000 and 400, we observed a clear difference between the release profile of tethered and trapped exosomes. We observed that tethered exosomes released relatively slower with more than 80% of the exosomes being retained even after 10 days. In contrast, almost all of the trapped exosomes were released from the hydrogels within 10 days. While a similar difference in the release behavior was observed for hydrogels with the monomer-to-crosslinker ratio of 8000, the tethered exosome released relatively faster due to low crosslinking density and only approximately 30% exosomes were retained after the 10-day period. This fast release of exosomes in low crosslinked hydrogels could be attributed to the larger mesh sizes that enable rapid diffusion and release of the entrapped cargo. These results highlight that the crosslinking density of the hydrogels can be tuned to ensure slower release kinetics for tethered exosomes.

Next, the elastic properties of exosome-tethered hydrogels were assessed. The elastic modulus of hydrogels in the biologically relevant stiffness range offers compliant interfaces with biological tissues. Young's modulus of exosome-tethered hydrogels with monomer-to-crosslinker ratios of 400, 4000, and 8000 was observed to be in the range of 2−8 kPa (Figure 2D). The original stress/strain curves are shown in Figure S5.

We also validated the membrane integrity of released exosomes from the Exo-tethered hydrogels of varying monomer-to-crosslinker ratios. The hydrogels were synthesized using calcein-labeled exosomes, and released exosomes were collected in a PBS buffer at 37 °C for 10 days. Fluorescence from calcein dye was analyzed using on-bead flow cytometry. The presence of an exosomal surface marker protein, CD63, allows the binding of exosomes onto anti-CD63 magnetic beads that can be analyzed using flow cytometry. Compared to the negative control of sonicated exosomes, calcein fluorescence signal in the released exosomes confirmed the integrity of released exosomes (Figures S7 and S8). Released exosomes from hydrogels of the monomer-to-crosslinker ratio of 8000 showed the highest fluorescence, while the lowest signal was observed for the monomer-to-crosslinker ratio of 400. It must be noted that due to the protein shedding of CD63 from the exosome membrane with

https://doi.org/10.1021/acs.biomac.1c01636
Biomacromolecules 2022, 23, 1713−1722

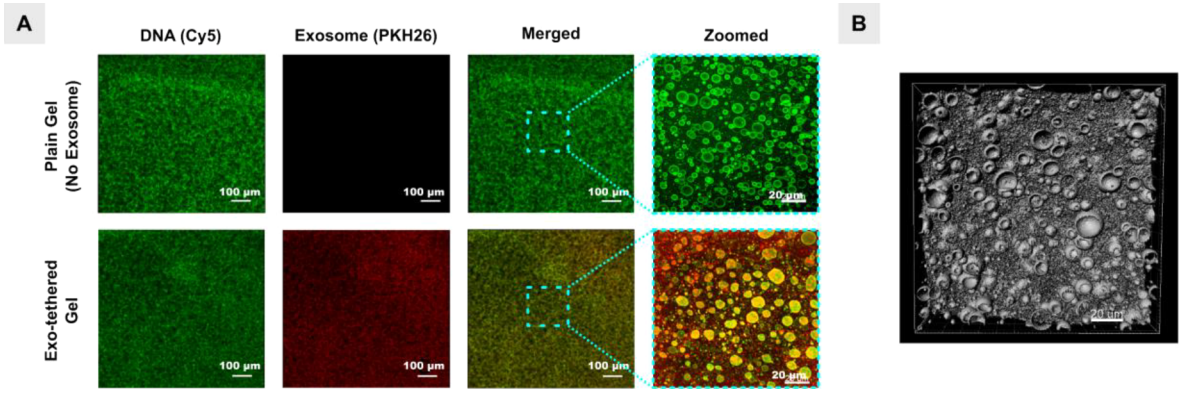

Figure 3. Characterization of exosome-tethered hydrogels with a monomer-to-crosslinker ratio (molar ratio of monomer to crosslinker) of 4000. (A) Confocal microscopy images showing exosomes tethered to the hydrogel. DNA tethers are in pseudo-green (Cy 5 label, Ex/Em: 650/670), and EVs, pseudo-red (PKH26 membrane label, Ex/Em:550/570). (B) Confocal image 3D reconstruction using Imaris (Oxford Instruments) software.

time,[46] quantitative comparison of exosomal membrane integrity is not possible. Going forward, we selected the monomer-to-crosslinker ratio of 4000 to ensure slower release kinetics for tethered exosomes without compromising the membrane integrity of the exosome membrane during polymerization. All the subsequent experiments were made such that 11.5 μg of exosomes was present in every 1 g of gel (wet wt.).

We then confirmed the tethering of exosomes inside the hydrogels using confocal microscopy. Exosomes were labeled with a lipophilic dye (PKH26), and a Cyanine 5 (Cy5) label was included in the tethered DNA macroinitiator species (Chol-dsDNA-Cy5-iBBr). The pregel solution was irradiated using blue light for up to 120 min to form the exosome-tethered hydrogels. Confocal images of the hydrogels post swelling (24 h incubation in PBS) showed the presence of both PKH26 and Cy5 dyes in the hydrogel (Figure 3A). We also observed smaller red dots upon 63× zoom that did not colocalize with the green signal (DNA tethers) and could be exosomes that are diffusing out. Using the confocal images, a 3D reconstruction was performed using Imaris software (Oxford Instruments) to assess the porosity of wet gels, which was determined to be 11.5 ± 6.5 μm using manual analysis of 20 random confocal images (Figure 3B). The pictures of the gels pre/postswelling and their swelling ratio are shown in Figure S9. DNA-tethered hydrogels prepared using PEO_{2000}-iBBr (95%) and Chol-dsDNA-Cy5-iBBr (5%) without exosomes served as the negative control and showed signal only for Cy5. After the entrapment of exosomes was confirmed, the monomer conversion was estimated using ^{1}H NMR spectroscopy. Hydrogels were prepared without exosomes or DNA, and the conversion of $PEGMA_{300}$ was measured over time. Gelation was observed at 110 min, and polymerization was continued for additional 10 min (Figure S3). We also verified the gel point using rheological assessment (Figure S6). However, please note that due to different apparatus utilized for rheological assessment, the gel point does not agree with the visual assessment. For subsequent studies, all hydrogels were prepared by exposure to blue light for 120 min to target approximately 60% monomer conversion. Prolonged polymerization time was avoided to minimize the exposure of exosomes to $PEGMA_{300}$, as methacrylate monomers can potentially be cytotoxic at higher concentrations.[47] To ensure that free copper ions were thoroughly removed, prior to cell-based studies, we performed a total of 4 washes with 0.02% EDTA in PBS, the first wash being immediate and followed by three more rinses.

Next, we assessed the efficacy of exosomes to effectively deliver a growth factor protein BMP2 using Exo-tethered hydrogels. Radiolabeled ^{125}I-BMP2 was loaded inside the lumen of exosomes as previously reported,[6] and the corresponding ^{125}I-Exo-tethered hydrogels were synthesized with a monomer-to-crosslinker ratio of 4000. Exosomes were radiolabeled as previously described.[38] The release kinetics of exosomes or free BMP2 were monitored over a period of 30 days (Figure 4), and the retained radioactivity in the gel was quantified at specific time points. Approximately, 98% of BMP2 protein and 57% of trapped BMP2-exosomes were released after 24 h (Figure 4; open symbols). In contrast,

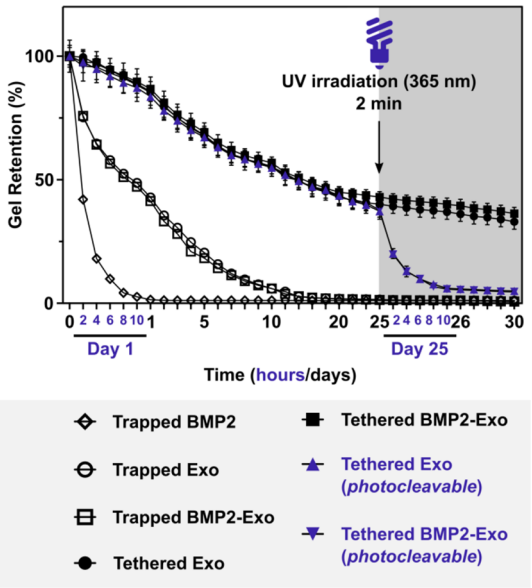

Figure 4. Release kinetics of radiolabeled exosomes from hydrogels with a monomer-to-crosslinker ratio of 4000. ^{125}I-exosomes or ^{125}I-BMP2 was utilized to study the release kinetics from PEO hydrogels over a period of 30 days. The gels were made such that every 1 g of gel contained 11.5 μg of exosome protein. The plot shows the release profile of physically entrapped and tethered exosomes from the hydrogels. Photocleavable hydrogels were irradiated with UV light for 2 min to cleave the DNA tether on day 25. Data were normalized to time 0 (% retained). Points indicate mean ± SEM (n = 3 replicates).

https://doi.org/10.1021/acs.biomac.1c01636
Biomacromolecules 2022, 23, 1713−1722

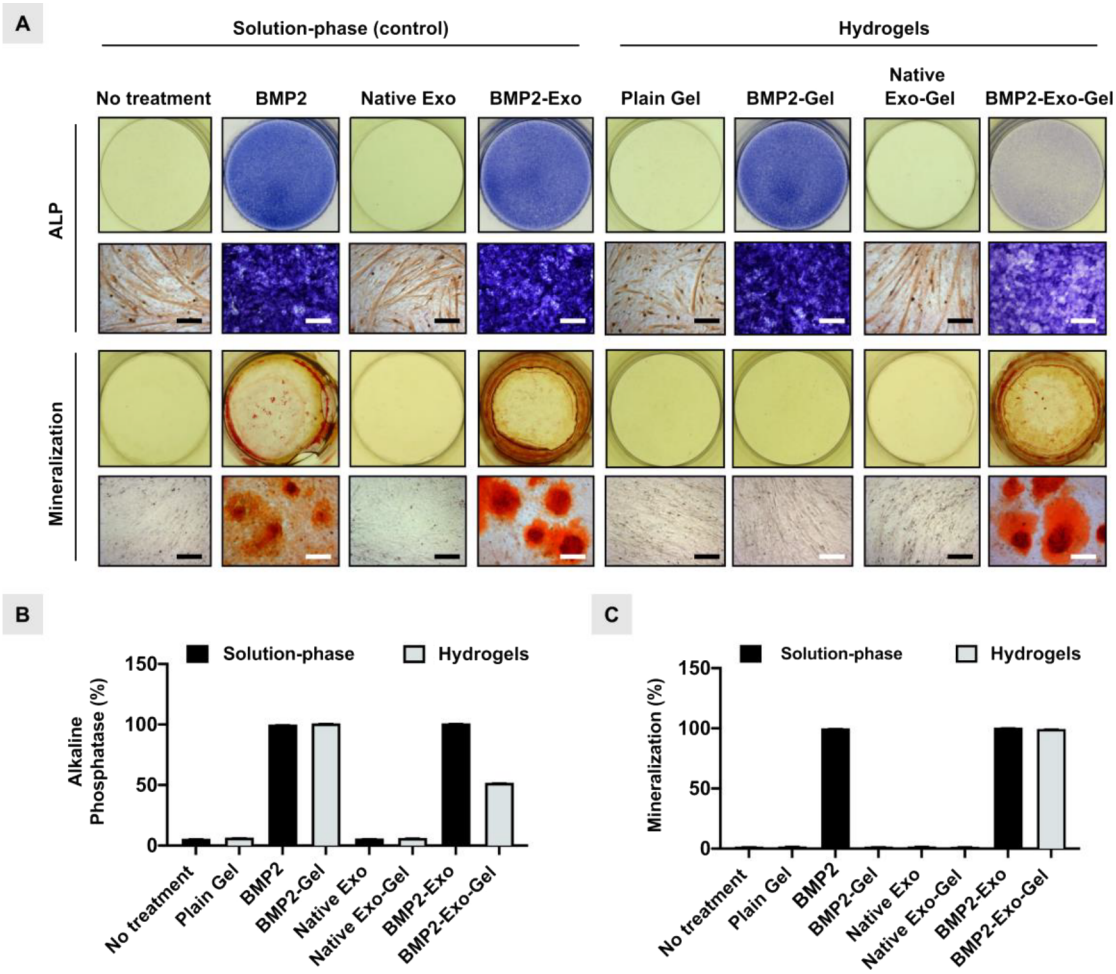

Figure 5. Osteogenic differentiation of C2C12 and MC3T3 cells using exosome-tethered hydrogels. (A) Photographs of C2C12 cells stained for ALP after 72 h and MC3T3 cells stained for mineralization after 28 days. C2C12 or MC3T3 cells were treated with the respective treatments either by directly adding them to the media every 72 h (solution-phase) or delivered via hydrogels added once on day 1. Scale bar = 50 μm. (B,C) Quantification of ALP expression and alizarin red staining. Bars indicate mean ± SEM (n = 3 independent experiments).

approximately 85% of tethered BMP2-exosomes were still retained inside the hydrogels after 24 h (Figure 4; closed symbols). After 10 days, more than 90% of the trapped BMP2-exosomes were released, while approximately only 45% release of tethered BMP2-exosomes was observed. At the end of the 30-day period, the hydrogels still retained approximately 30% of the tethered BMP2-exosomes. The release profile of the photocleavable exosome-tethered hydrogels was also assessed, and similar kinetics were observed. On day 25, these hydrogels were irradiated with UV light (365 nm) for 2 min to cleave the DNA tethers from the exosome surface. More than 95% of the remaining exosomes were released in the next 8 h. These results highlight the excellent temporal control over the release of tethered exosomes. We observed no significant difference in the release profile of native and BMP2-loaded exosomes during this study.

To evaluate the bioactivity of exosome-tethered hydrogels, BMP2-loaded exosomes were used to prepare the hydrogels. The in vitro osteoinduction due to released BMP2-exosomes with C2C12 cells was assessed. Two bone formation markers, ALP and mineral deposits, were analyzed. ALP is an early bone differentiation marker, and mineral deposits are late bone differentiation markers. The ALP assay was concluded in 72 h without any media change. The cells treated with BMP2 and BMP2-exosomes, both in the solution phase (control) and through hydrogels, resulted in osteogenic differentiation of C2C12 cells as evidenced by upregulation in ALP expression (Figure 5A,B). The descriptions of hydrogel treatments are mentioned in Table S2.

The mineralization assay, using MC3T3 cells, was performed over a period of 28 days with media changed every 72 h. Then, 100 ng/mL BMP2 was supplemented during every media change for experiments involving solution-phase assays. In contrast, the cells incubated with hydrogels did not receive any additional BMP2 with the fresh media, and therefore, the bone differentiation relied only on BMP2 being released from the hydrogel. For mineral deposits to form, a continuous stimulation by BMP2 is critical for the cells to differentiate into bone-like cells. Cells that received solution-phase BMP2 every 72 h or treated with hydrogel BMP2-exosomes on day 1 (with no subsequent BMP2 supplementation) resulted in mineral deposits. This indicates that when tethered to the hydrogels, the BMP2-exosomes were slowly released into the media that effect cell differentiation (Figure 5A,C). However, physically entrapped BMP2 did not result in the formation of mineral deposits. Next, we wanted to check whether the presence of a photocleavable (pc) group affects BMP2-exosome activity in the gels. Hence, we prepared pc-BMP2-

https://doi.org/10.1021/acs.biomac.1c01636
Biomacromolecules 2022, 23, 1713−1722

exosome-tethered and assessed their potential to induce ALP expression in C2C12 cells after irradiating the gels at 365 nm for 2 min. The results indicate that 2 min exposure to 365 nm did not affect the osteogenic potential of BMP2-exosomes (Figure S10).

The first generation of exosome gels reported here has certain limitations that can be addressed in follow-up studies. First, while the exosome gels can be surgically implanted, an injectable version of the same would be more desirable for minimally invasive therapeutics. We anticipate PEO gels to degrade in the body by ester hydrolysis or by ROS generated during inflammatory reaction surrounding the gel implantation site similar to PEG gels reported in the literature.[48] Second, we have explored only one type of polymeric material, i.e., PEO hydrogels, but other types of hydrogels such as zwitterionic hydrogels could potentially have more clinical applications. Third, we did not explore the full extent of crosslinking density possible in the PEO gel system. Young's modulus of biological tissues ranges between 0.1 kPa and 1 MPa, and therefore, having hydrogels within this whole spectrum could ultimately be beneficial for tissue-specific applications.

CONCLUSIONS

We report the development of biocompatible exosome-tethered hydrogels by photoinduced ATRP for the controlled release of exosomes. Blue-light-mediated photoinduced ATRP is highly biocompatible and permits the use of synthetic polymers for hydrogels containing exosomes. Further, cholesterol-modified DNA tethers are shown to be advantageous compared to the physical entrapment of exosomes in these hydrogels. Hydrogels tethered with BMP2-loaded exosomes have the potential to stimulate osteogenic differentiation in vitro. Importantly, the DNA tethers can include photocleavable linkers that are compatible with the polymerization process and allow for temporal control over exosome release. The photomediated release of exosomes from the hydrogels serves as a proof-of-principle for the stimuli-responsive exosome delivery strategy. We envisage the use of other responsive cleavable linkers that may be readily incorporated into DNA, and further tuning of the release through stimuli-responsive crosslinkers. Other release strategies that depend on small molecules or tissue-specific physiological conditions[49] would further expand the utility and applications of the DNA-tethered exosome hydrogels that we describe here.

ASSOCIATED CONTENT

Supporting Information

The Supporting Information is available free of charge at https://pubs.acs.org/doi/10.1021/acs.biomac.1c01636.

Cell culture; exosome isolation and characterization; DNA synthesis; preparation and characterization of BMP2-loaded exosomes, exosome macroinitiator and hydrogels by ATRP; cytotoxicity and cell proliferation assay; release kinetic studies; and supplementary figures and tables (PDF)

AUTHOR INFORMATION

Corresponding Authors

Subha R. Das − *Department of Chemistry and The Center for Nucleic Acids Science & Technology, Carnegie Mellon University, Pittsburgh, Pennsylvania 15213, United States;* orcid.org/0000-0002-5353-0422; Email: srdas@andrew.cmu.edu

Phil G. Campbell − *Department of Biomedical Engineering and Engineering Research Accelerator, Carnegie Mellon University, Pittsburgh, Pennsylvania 15213, United States;* Email: pcampbel@cs.cmu.edu

Krzysztof Matyjaszewski − *Department of Chemistry, Carnegie Mellon University, Pittsburgh, Pennsylvania 15213, United States;* orcid.org/0000-0003-1960-3402; Email: km3b@andrew.cmu.edu

Authors

Saigopalakrishna S. Yerneni − *Department of Biomedical Engineering and Engineering Research Accelerator, Carnegie Mellon University, Pittsburgh, Pennsylvania 15213, United States*

Sushil Lathwal − *Department of Chemistry and The Center for Nucleic Acids Science & Technology, Carnegie Mellon University, Pittsburgh, Pennsylvania 15213, United States*

Julia Cuthbert − *Department of Chemistry, Carnegie Mellon University, Pittsburgh, Pennsylvania 15213, United States*

Kriti Kapil − *Department of Chemistry, Carnegie Mellon University, Pittsburgh, Pennsylvania 15213, United States*

Grzegorz Szczepaniak − *Department of Chemistry, Carnegie Mellon University, Pittsburgh, Pennsylvania 15213, United States;* orcid.org/0000-0002-0355-9542

Jaepil Jeong − *Department of Chemistry and The Center for Nucleic Acids Science & Technology, Carnegie Mellon University, Pittsburgh, Pennsylvania 15213, United States*

Complete contact information is available at: https://pubs.acs.org/10.1021/acs.biomac.1c01636

Author Contributions

S.S.Y. and S.L. contributed equally to this work as co-first authors. The manuscript was written through the contributions of all authors. All authors have given approval to the final version of the manuscript.

Funding

This work was supported by NSF (DMR 1501324 and DMR 2202747), DTRA (HDTRA1-20-1-0014), and NIH (R21AR072954-01).

Notes

The authors declare no competing financial interest.

REFERENCES

(1) Yáñez-Mó, M.; Siljander, P. R. M.; Andreu, Z.; Bedina Zavec, A.; Borràs, F. E.; Buzas, E. I.; Buzas, K.; Casal, E.; Cappello, F.; Carvalho, J.; Colás, E.; Cordeiro-da Silva, A.; Fais, S.; Falcon-Perez, J. M.; Ghobrial, I. M.; Giebel, B.; Gimona, M.; Graner, M.; Gursel, I.; Gursel, M.; Heegaard, N. H. H.; Hendrix, A.; Kierulf, P.; Kokubun, K.; Kosanovic, M.; Kralj-Iglic, V.; Krämer-Albers, E.-M.; Laitinen, S.; Lässer, C.; Lener, T.; Ligeti, E.; Linē, A.; Lipps, G.; Llorente, A.; Lötvall, J.; Manček-Keber, M.; Marcilla, A.; Mittelbrunn, M.; Nazarenko, I.; Nolte-'t Hoen, E. N. M.; Nyman, T. A.; O'Driscoll, L.; Olivan, M.; Oliveira, C.; Pállinger, É.; del Portillo, H. A.; Reventós, J.; Rigau, M.; Rohde, E.; Sammar, M.; Sánchez-Madrid, F.; Santarém, N.; Schallmoser, K.; Stampe Ostenfeld, M.; Stoorvogel, W.; Stukelj, R.; Van der Grein, S. G.; Helena Vasconcelos, M.; Wauben, M. H. M.; De Wever, O. Biological properties of extracellular vesicles and their physiological functions. *J. Extracell. Vesicles* **2015**, *4*, 27066.

(2) El Andaloussi, S.; Mäger, I.; Breakefield, X. O.; Wood, M. J. A. Extracellular vesicles: biology and emerging therapeutic opportunities. *Nat. Rev. Drug Discovery* **2013**, *12*, 347−357.

(3) Maas, S. L. N.; Breakefield, X. O.; Weaver, A. M. Extracellular Vesicles: Unique Intercellular Delivery Vehicles. *Trends Cell Biol.* **2017**, *27*, 172−188.
(4) Armstrong, J. P. K.; Holme, M. N.; Stevens, M. M. Re-Engineering Extracellular Vesicles as Smart Nanoscale Therapeutics. *ACS Nano* **2017**, *11*, 69−83.
(5) Yerneni, S. S.; Whiteside, T. L.; Weiss, L. E.; Campbell, P. G. Bioprinting exosome-like extracellular vesicle microenvironments. *Bioprinting* **2019**, *13*, No. e00041.
(6) Yerneni, S. S.; Adamik, J.; Weiss, L. E.; Campbell, P. G. Cell trafficking and regulation of osteoblastogenesis by extracellular vesicle associated bone morphogenetic protein 2. *J. Extracell. Vesicles* **2021**, *10*, No. e12155.
(7) Lathwal, S.; Yerneni Saigopalakrishna, S.; Boye, S.; Muza Upenyu, L.; Takahashi, S.; Sugimoto, N.; Lederer, A.; Das Subha, R.; Campbell Phil, G.; Matyjaszewski, K. Engineering exosome polymer hybrids by atom transfer radical polymerization. *Proc. Natl. Acad. Sci. U. S. A.* **2021**, *118*, No. e2020241118.
(8) Yerneni, S. S.; Lathwal, S.; Shrestha, P.; Shirwan, H.; Matyjaszewski, K.; Weiss, L.; Yolcu, E. S.; Campbell, P. G.; Das, S. R. Rapid On-Demand Extracellular Vesicle Augmentation with Versatile Oligonucleotide Tethers. *ACS Nano* **2019**, *13*, 10555−10565.
(9) van der Meel, R.; Fens, M. H. A. M.; Vader, P.; van Solinge, W. W.; Eniola-Adefeso, O.; Schiffelers, R. M. Extracellular vesicles as drug delivery systems: Lessons from the liposome field. *J. Controlled Release* **2014**, *195*, 72−85.
(10) Lener, T.; Gimona, M.; Aigner, L.; Börger, V.; Buzas, E.; Camussi, G.; Chaput, N.; Chatterjee, D.; Court, F. A.; de Portillo, H. A.; O'Driscoll, L.; Fais, S.; Falcon-Perez, J. M.; Felderhoff-Mueser, U.; Fraile, L.; Gho, Y. S.; Görgens, A.; Gupta, R. C.; Hendrix, A.; Hermann, D. M.; Hill, A. F.; Hochberg, F.; Horn, P. A.; de Kleijn, D.; Kordelas, L.; Kramer, B. W.; Krämer-Albers, E.-M.; Laner-Plamberger, S.; Laitinen, S.; Leonardi, T.; Lorenowicz, M. J.; Lim, S. K.; Lötvall, J.; Maguire, C. A.; Marcilla, A.; Nazarenko, I.; Ochiya, T.; Patel, T.; Pedersen, S.; Pocsfalvi, G.; Pluchino, S.; Quesenberry, P.; Reischl, I. G.; Rivera, F. J.; Sanzenbacher, R.; Schallmoser, K.; Slaper-Cortenbach, I.; Strunk, D.; Tonn, T.; Vader, P.; van Balkom, B. W. M.; Wauben, M.; Andaloussi, S. E.; Théry, C.; Rohde, E.; Giebel, B. Applying extracellular vesicles based therapeutics in clinical trials − an ISEV position paper. *J. Extracell. Vesicles* **2015**, *4*, 30087.
(11) Xing, Y.; Yerneni, S. S.; Wang, W.; Taylor, R. E.; Campbell, P. G.; Ren, X. Engineering pro-angiogenic biomaterials via chemo-selective extracellular vesicle immobilization. *Biomaterials* **2022**, *281*, No. 121357.
(12) Yamashita, T.; Takahashi, Y.; Takakura, Y. Possibility of Exosome-Based Therapeutics and Challenges in Production of Exosomes Eligible for Therapeutic Application. *Biol. Pharm. Bull.* **2018**, *41*, 835−842.
(13) Kearney, C. J.; Mooney, D. J. Macroscale delivery systems for molecular and cellular payloads. *Nat. Mater.* **2013**, *12*, 1004−1017.
(14) Riau, A. K.; Ong, H. S.; Yam, G. H. F.; Mehta, J. S. Sustained Delivery System for Stem Cell-Derived Exosomes. *Front. Pharmacol.* **2019**, *10*, 1368.
(15) Peppas, N. A.; Bures, P.; Leobandung, W.; Ichikawa, H. Hydrogels in pharmaceutical formulations. *Eur. J. Pharm. Biopharm.* **2000**, *50*, 27−46.
(16) Mandal, A.; Clegg, J. R.; Anselmo, A. C.; Mitragotri, S. Hydrogels in the clinic. *Bioeng. Transl. Med.* **2020**, *5*, No. e10158.
(17) Lin, C.-C.; Anseth, K. S. PEG Hydrogels for the Controlled Release of Biomolecules in Regenerative Medicine. *Pharm. Res.* **2009**, *26*, 631−643.
(18) Yang, G.; Chen, Q.; Wen, D.; Chen, Z.; Wang, J.; Chen, G.; Wang, Z.; Zhang, X.; Zhang, Y.; Hu, Q.; Zhang, L.; Gu, Z. A Therapeutic Microneedle Patch Made from Hair-Derived Keratin for Promoting Hair Regrowth. *ACS Nano* **2019**, *13*, 4354−4360.
(19) Akbari, A.; Jabbari, N.; Sharifi, R.; Ahmadi, M.; Vahhabi, A.; Seyedzadeh, S. J.; Nawaz, M.; Szafert, S.; Mahmoodi, M.; Jabbari, E.; Asghari, R.; Rezaie, J. Free and hydrogel encapsulated exosome-based therapies in regenerative medicine. *Life Sci.* **2020**, *249*, No. 117447.
(20) Pishavar, E.; Luo, H.; Naserifar, M.; Hashemi, M.; Toosi, S.; Atala, A.; Ramakrishna, S.; Behravan, J. Advanced Hydrogels as Exosome Delivery Systems for Osteogenic Differentiation of MSCs: Application in Bone Regeneration. *Int. J. Mol. Sci.* **2021**, *22*, 6203.
(21) Enciso, A. E.; Fu, L.; Russell, A. J.; Matyjaszewski, K. A Breathing Atom-Transfer Radical Polymerization: Fully Oxygen-Tolerant Polymerization Inspired by Aerobic Respiration of Cells. *Angew. Chem., Int. Ed.* **2018**, *57*, 933−936.
(22) Fu, L.; Wang, Z.; Lathwal, S.; Enciso, A. E.; Simakova, A.; Das, S. R.; Russell, A. J.; Matyjaszewski, K. Synthesis of Polymer Bioconjugates via Photoinduced Atom Transfer Radical Polymerization under Blue Light Irradiation. *ACS Macro Lett.* **2018**, *7*, 1248−1253.
(23) Matyjaszewski, K. Advanced Materials by Atom Transfer Radical Polymerization. *Adv. Mater.* **2018**, *30*, No. 1706441.
(24) Siegwart, D. J.; Oh, J. K.; Matyjaszewski, K. ATRP in the design of functional materials for biomedical applications. *Prog. Polym. Sci.* **2012**, *37*, 18−37.
(25) Baker, S. L.; Kaupbayeva, B.; Lathwal, S.; Das, S. R.; Russell, A. J.; Matyjaszewski, K. Atom Transfer Radical Polymerization for Biorelated Hybrid Materials. *Biomacromolecules* **2019**, *20*, 4272−4298.
(26) Chen, C.; Ng, D. Y. W.; Weil, T. Polymer bioconjugates: Modern design concepts toward precision hybrid materials. *Prog. Polym. Sci.* **2020**, *105*, No. 101241.
(27) Matyjaszewski, K. Atom Transfer Radical Polymerization (ATRP): Current Status and Future Perspectives. *Macromolecules* **2012**, *45*, 4015−4039.
(28) Corrigan, N.; Jung, K.; Moad, G.; Hawker, C. J.; Matyjaszewski, K.; Boyer, C. Reversible-deactivation radical polymerization (Controlled/living radical polymerization): From discovery to materials design and applications. *Prog. Polym. Sci.* **2020**, *111*, No. 101311.
(29) Parkatzidis, K.; Wang, H. S.; Truong, N. P.; Anastasaki, A. Recent Developments and Future Challenges in Controlled Radical Polymerization: A 2020 Update. *Chem* **2020**, *6*, 1575−1588.
(30) Ludwig, N.; Razzo, B. M.; Yerneni, S. S.; Whiteside, T. L. Optimization of cell culture conditions for exosome isolation using mini-size exclusion chromatography (mini-SEC). *Exp. Cell Res.* **2019**, *378*, 149−157.
(31) Ludwig, N.; Yerneni, S. S.; Razzo, B. M.; Whiteside, T. L. Exosomes from HNSCC Promote Angiogenesis through Reprogramming of Endothelial Cells. *Mol. Cancer Res.* **2018**, *16*, 1798−1808.
(32) Hong, C.-S.; Sharma, P.; Yerneni, S. S.; Simms, P.; Jackson, E. K.; Whiteside, T. L.; Boyiadzis, M. Circulating exosomes carrying an immunosuppressive cargo interfere with cellular immunotherapy in acute myeloid leukemia. *Sci. Rep.* **2017**, *7*, 14684.
(33) Yerneni Saigopalakrishna, S.; Werner, S.; Azambuja Juliana, H.; Ludwig, N.; Eutsey, R.; Aggarwal Surya, D.; Lucas Peter, C.; Bailey, N.; Whiteside Theresa, L.; Campbell Phil, G.; Hiller, N. L.; McDaniel Larry, S. Pneumococcal Extracellular Vesicles Modulate Host Immunity. *MBio* **2021**, *12*, e01657−e01621.
(34) Pan, X.; Lathwal, S.; Mack, S.; Yan, J.; Das, S. R.; Matyjaszewski, K. Automated Synthesis of Well-Defined Polymers and Biohybrids by Atom Transfer Radical Polymerization Using a DNA Synthesizer. *Angew. Chem., Int. Ed.* **2017**, *56*, 2740−2743.
(35) Haney, M. J.; Klyachko, N. L.; Zhao, Y.; Gupta, R.; Plotnikova, E. G.; He, Z.; Patel, T.; Piroyan, A.; Sokolsky, M.; Kabanov, A. V.; Batrakova, E. V. Exosomes as drug delivery vehicles for Parkinson's disease therapy. *J. Controlled Release* **2015**, *207*, 18−30.
(36) Cuthbert, J.; Yerneni, S. S.; Sun, M.; Fu, T.; Matyjaszewski, K. Degradable Polymer Stars Based on Tannic Acid Cores by ATRP. *Polymer* **2019**, *11*, 752.
(37) Kassick, A. J.; Allen, H. N.; Yerneni, S. S.; Pary, F.; Kovaliov, M.; Cheng, C.; Pravetoni, M.; Tomycz, N. D.; Whiting, D. M.; Nelson, T. L.; Feasel, M.; Campbell, P. G.; Kolber, B.; Averick, S. Covalent Poly(lactic acid) Nanoparticles for the Sustained Delivery of Naloxone. *ACS Appl. Bio Mater.* **2019**, *2*, 3418−3428.

https://doi.org/10.1021/acs.biomac.1c01636
Biomacromolecules 2022, 23, 1713−1722

(38) Yerneni, S. S.; Solomon, T.; Smith, J.; Campbell, P. G. Radioiodination of extravesicular surface constituents to study the biocorona, cell trafficking and storage stability of extracellular vesicles. *Biochim. Biophys. Acta* **2022**, *1866*, No. 130069.
(39) Gray, W. D.; Mitchell, A. J.; Searles, C. D. An accurate, precise method for general labeling of extracellular vesicles. *MethodsX* **2015**, *2*, 360−367.
(40) Theodoraki, M.-N.; Yerneni, S. S.; Hoffmann, T. K.; Gooding, W. E.; Whiteside, T. L. Clinical Significance of PD-L1+ Exosomes in Plasma of Head and Neck Cancer Patients. *Clin. Cancer Res.* **2018**, *24*, 896−905.
(41) Kassick, A. J.; Yerneni, S. S.; Gottlieb, E.; Cartieri, F.; Peng, Y.; Mao, G.; Kharlamov, A.; Miller, M. C.; Xu, C.; Oh, M.; Kowalewski, T.; Cheng, B.; Campbell, P. G.; Averick, S. Osteoconductive Enhancement of Polyether Ether Ketone: A Mild Covalent Surface Modification Approach. *ACS Appl. Bio Mater.* **2018**, *1*, 1047−1055.
(42) Pan, X.; Tasdelen, M. A.; Laun, J.; Junkers, T.; Yagci, Y.; Matyjaszewski, K. Photomediated controlled radical polymerization. *Prog. Polym. Sci.* **2016**, *62*, 73−125.
(43) Szczepaniak, G.; Fu, L.; Jafari, H.; Kapil, K.; Matyjaszewski, K. Making ATRP More Practical: Oxygen Tolerance. *Acc. Chem. Res.* **2021**, *54*, 1779−1790.
(44) Il'ichev, Y. V.; Schwörer, M. A.; Wirz, J. Photochemical Reaction Mechanisms of 2-Nitrobenzyl Compounds: Methyl Ethers and Caged ATP. *J. Am. Chem. Soc.* **2004**, *126*, 4581−4595.
(45) Bai, X.; Li, Z.; Jockusch, S.; Turro Nicholas, J.; Ju, J. Photocleavage of a 2-nitrobenzyl linker bridging a fluorophore to the 5′ end of DNA. *Proc. Natl. Acad. Sci. U. S. A.* **2003**, *100*, 409−413.
(46) Lee, M.; Ban, J.-J.; Im, W.; Kim, M. Influence of storage condition on exosome recovery. *Biotechnol. Bioprocess Eng.* **2016**, *21*, 299−304.
(47) Geng, J.; Li, W.; Zhang, Y.; Thottappillil, N.; Clavadetscher, J.; Lilienkampf, A.; Bradley, M. Radical polymerization inside living cells. *Nat. Chem.* **2019**, *11*, 578−586.
(48) Reid, B.; Gibson, M.; Singh, A.; Taube, J.; Furlong, C.; Murcia, M.; Elisseeff, J. PEG hydrogel degradation and the role of the surrounding tissue environment. *J. Tissue Eng. Regener. Med.* **2015**, *9*, 315−318.
(49) Culver, H. R.; Clegg, J. R.; Peppas, N. A. Analyte-Responsive Hydrogels: Intelligent Materials for Biosensing and Drug Delivery. *Acc. Chem. Res.* **2017**, *50*, 170−178.

https://doi.org/10.1021/acs.biomac.1c01636
Biomacromolecules 2022, 23, 1713−1722